Development of TiN Vacuum-Gap Capacitor Lumped-Element Kinetic Inductance Detectors

Faouzi Boussaha, Samir Beldi, Alessandro Monfardini, Jie Hu, Martino Calvo, Christine Chaumont, Florence Lévy-Bertrand, Thibaut Vacelet, Alessandro Traini, Josiane Firminy, et al.

Development of TiN Vacuum-Gap Capacitor Lumped Element Kinetic Inductance Detectors

Faouzi Boussaha[1] • Samir Beldi[1] • Alessandro Monfardini[2] • Jie Hu[3] • Martino Calvo[2] • Christine Chaumont[1] • Florence Levy-Bertrand[2] • Thibaut Vacelet[1] • Alessandro Traini[3] • Josiane Firminy[1] • Michel Piat[3] • Florent Reix[1]

1. *GEPI, Observatoire de Paris, Université PSL, CNRS, 75014 Paris, France*
2. *Université de Grenoble Alpes, CNRS, Grenoble INP, Institut Néel, 38000 Grenoble – France*
3. *Laboratoire AstroParticule et Cosmologie, Université Paris Diderot 75013 Paris, France*

Abstract
We report on the implementation of a vacuum parallel-plate capacitor manufactured using a straightforward process that allows to accurately set nanoscale vacuum gaps in order to reach fairly large capacitances with small footprints. Vacuum gaps between 150 and 300 nm have been achieved. To prevent native oxides and therefore two-level systems (TLS), both electrodes are made of TiN-based layers. We implemented the vacuum parallel-plate capacitors into lumped-element kinetic inductance detectors and compared their performances to standard interdigitated capacitor-based detectors. The vacuum capacitor detectors achieved higher quality factors (up to 1.1×10^6) and lower frequency noise (2.8 ± 0.5 Hz²/Hz at 10 Hz). Furthermore, we demonstrate that the noise generated within the meander of the lumped-element kinetic inductance detector can be as important as the one generated in the capacitance.

Keywords Kinetic inductance detector, vacuum gap capacitor, TiN electrodes.

1 Introduction

Dielectric materials used to build capacitor-based superconducting devices such as lumped element kinetic inductance detectors (LEKIDs) and quantum bits (qubits) feature an intrinsic noise due to two-level systems (TLS). This noise is generated at metal/dielectric interfaces, particularly when dielectrics are amorphous, as well as in the bulk substrate causing fluctuations in the dielectric constant [1] and therefore in the capacitance value, which in turn

induces random changes in frequency. In fact, likely because of TLS, the capacitor has been identified as the main source of excess noise [2] in KIDs [3] and decoherence in Josephson quantum computing devices [4]. To attempt to reduce TLS, several groups are investigating the use of dielectrics featuring a low number of defects such as monocrystalline silicon [5], a-Si:H [6] or SiN_x [7]. However, they remain dielectrics and would not guarantee a substantial gain in performance. The ideal solution is the use of capacitors without dielectric materials. However, removing solid dielectrics is challenging as it would necessarily require suspended structures with very tight vacuum gaps between superconducting plates to reach a quite high capacitance with a small footprint. K. Cicak et al. [8] succeeded in implementing Al vacuum parallel-plate-capacitor resonators. These resonators exhibited a high internal quality factor (Q_i~1.7×10^5) which, however, is similar to the best interdigitated capacitor-based resonators [9]. As they stated, it is likely due to native oxides (AlO_x) which is formed on inner electrode surfaces and support structures. Furthermore, such complex structure would complicate further the development of LEKID arrays where a large number of detectors should be patterned. In this work, we present TiN vacuum-gap capacitor LEKIDs implemented thanks to a quite simple fabrication process.

2 Vacuum capacitor LEKID design

Our LEKIDs are designed to resonate within the 1-2 GHz frequency band and have been simulated using same substrate and superconducting layer parameters reported elsewhere [10-11]. Figure 1 shows the sketch of the resonator that consists of a TiN meandered inductor connected in parallel to the vacuum parallel plate capacitor, inductively coupled to a 50 Ω CPW feedline. The meander size patterned from 60 nm-thick TiN is 610×560 μm. We set a 20 μm-gap between 2.5 μm-width strips. For this study, we choose to use stable stoichiometric TiN films with critical temperature T_c around 4.6 K and resistivity ρ~140 μΩ.cm. Using Mattis-Bardeen relationship [11], we estimate the sheet kinetic inductance $L_{k\square}$ to be 7-8 pH/□. The TiN total inductance (L_k+$L_{geometric}$) is ~62 nH with L_k~55 nH. The capacitor consists of a solid rectangle bottom electrode and a comb-shaped upper-electrode. It is made up of N parallel bridges connected at their respective extremities by two perpendicular strips of a few μm width that serves also as resting points on the substrate. To avoid native oxide that can alter the quality factor and promote TLS, both upper and bottom-electrodes are also patterned from pure TiN (i.e. no other type of superconducting material has been added) or TiN-

Development of TiN Vacuum-Gap Capacitor Lumped Element Kinetic Inductance Detectors

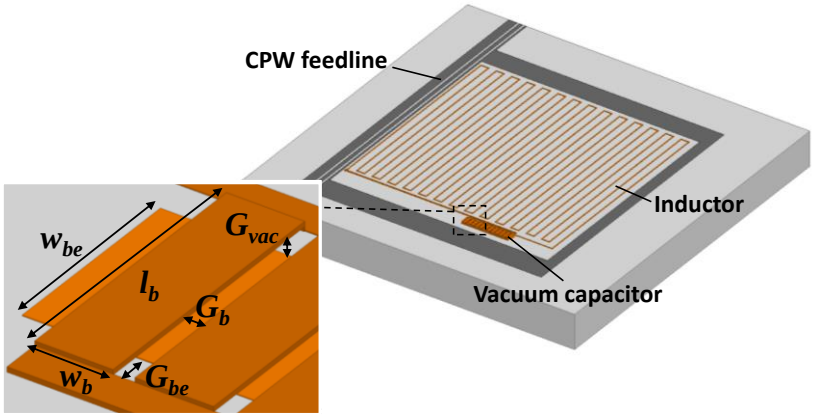

Fig. 1 Sketch of the vacuum capacitor LEKID.The gap between the bottom electrode and parallel strip edges G_{be} is 1.5 μm. The gap between bridges is fixed at G_b=4μm.

based multilayers which, being nitrides, do not oxide easily compared to Nb or Al. The choice between pure TiN and TiN-based multilayer depends on the critical temperature along with the mechanical stress criteria as presented below. The capacitance value is calculated using:

$$C_{vac} = \varepsilon_0 l_{eff} w_{be} / d \quad (1)$$

where ε_0 is the permittivity of the vacuum, d is the vacuum gap between electrodes, w_{be} is the bottom electrode width and l_{eff} is the capacitor effective length given by:

$$l_{eff} = N w_b + (N-1) G_b \quad (2)$$

where N is the bridge number, G_b is the gap between bridges and w_b the width of each bridge. Thus, the capacitance value can be tuned by varying dimension and number of bridges. As an example, Fig. 2 shows the simulated forward transmission S_{21} response of the feedline and the current density within the LEKID whose vacuum capacitor consists of four $l_b \times w_b$=32×12 μm bridges, using the electromagnetic simulation package SONNET [12]. The vacuum gap and bottom electrode width are set to d=200 nm and w_{be}=23 μm, respectively. This leads to a calculated capacitor of C_{vac}=48.8 fF. The simulation is performed with a substrate tangent loss ($tan\delta$) set at 2×10^{-6}. The

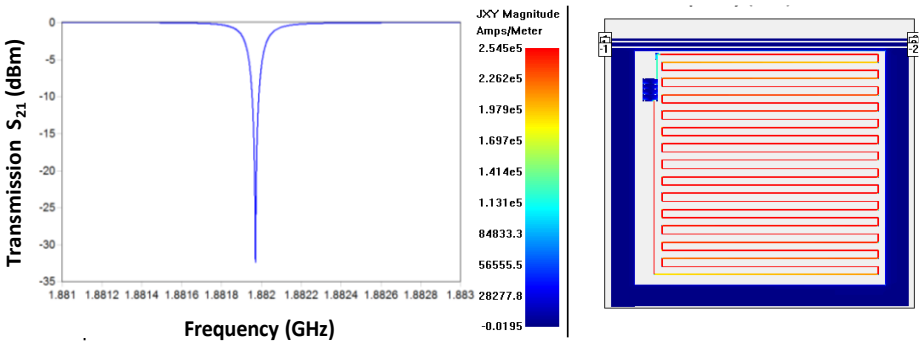

Fig. 2 Sonnet simulation of a vacuum capacitor LEKID.

vacuum capacitor LEKID resonates at f_{sim}=1.881 GHz and shows an internal and coupling quality factors of Q_i~7.8×10^5 and Q_c~1.9×10^4, respectively. For comparison, we also designed an interdigitated capacitor-based LEKID. We replace the vacuum capacitor by an interdigitated capacitor featuring 3.5 strips of 598 µm length, 2.5 µm width and 5 µm gap which makes the LEKID resonating at the same frequency (1.883 GHz). Using same superconductor and substrate parameters, we obtain a weaker Q_i of 4.5×10^5 but nevertheless in the same order of magnitude and a rather similar quality coupling factor Q_c of 2.1×10^4. We designed and fabricated four LEKID arrays: two with vacuum capacitors (VC) and two with interdigitated capacitors (IDC). For each design (VC or IDC) one array was deposited onto sapphire substrate and one onto silicon substrate. Each array consists of 25 resonators with an identical inductive meander but with different capacitors to tune the resonance frequencies. We varied multiple parameters of the vacuum capacitors to study their influence on the production process reliability. The number of bridges N was varied from 1 to 34, the length of the bridge l_b from 32 to 35 µm, the width of the bridge w_b from 9 to 18 µm. The bottom electrode width w_{be} was set to 23 or 26 µm. The vacuum gap (d=200 nm) and interdigitated capacitors were designed to achieve 14 to 311 fF and 71 to 368 fF, respectively. The calculated resonance frequencies range from ~ 1 GHz to 2.3 GHz.

3 Superconducting TiN suspended electrodes

The most delicate part of this study was the fabrication of TiN vacuum capacitors which required to implement a quite innovative process. The devices are patterned using sputter deposition, optical lithography and lift-off techniques. We used high resistivity (>15 kΩ.cm) and <100>-oriented silicon

Development of TiN Vacuum-Gap Capacitor Lumped Element Kinetic Inductance Detectors

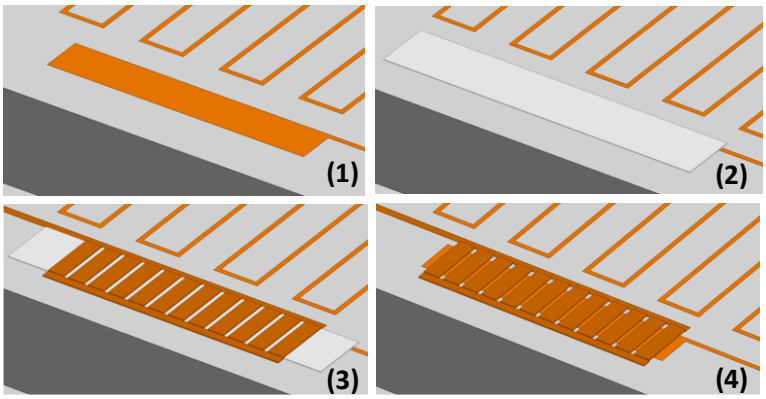

Fig. 3 Sketch of the fabrication process: (1) TiN meander and bottom electrode deposition, (2) Al layer deposition (the sacrificial layer), (3) upper-electrode deposition (4) Al dissolution.

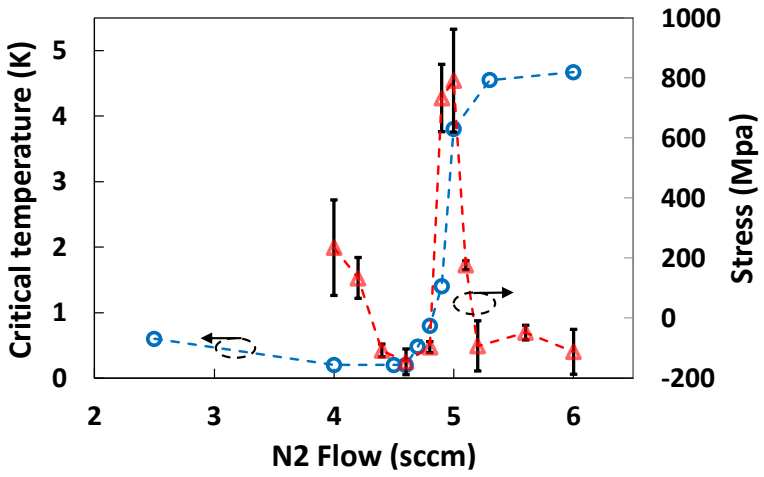

Fig. 4 Measured critical temperature and stress of TiN layers as a function of N_2 flow rate. Stresses were measured using a mechanical profilometer. It consists of measuring the curvature of the substrate prior to and after the TiN layer deposition. The stress value is calculated using the bending plate method, based on the change in the curvature. For each measured stress, we performed several scans along different directions and took mean values. Temperatures were extracted using 4-point probe measurements.

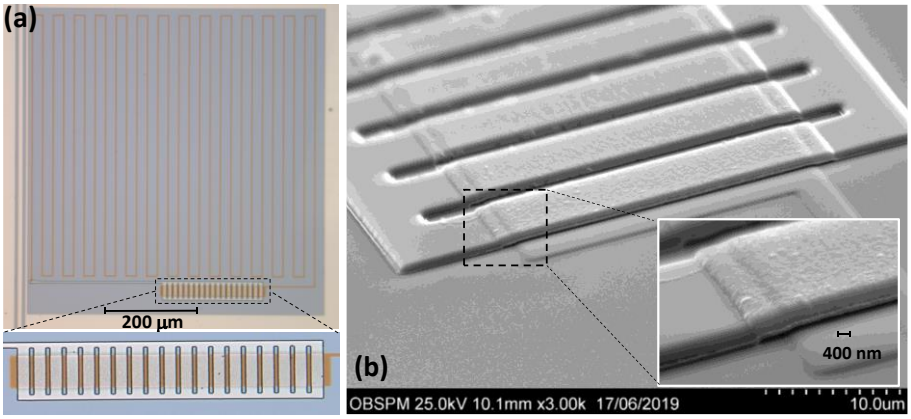

Fig. 5 (a) optical and (b) scanning electron microscope (SEM) photos of a vacuum parallel plate capacitor made of TiN/Nb upper-electrode with bridge size $l_b \times w_b = 35 \times 9 \mu m$ and 200 nm vacuum gap.

and 99.999% high-purity and c-plane monocrystalline sapphire substrates. All substrates were 50 mm in diameter and 280 μm-thick. Figure 3 depicts the fabrication process. First, the inductive meanders and lower rectangular electrodes are patterned from a 60 nm-thick TiN layer which is deposited starting from a 99.995 % titanium target. Then, the CPW feedline is made out using 100 nm-thick niobium (Nb) (not shown). The final step is building the vacuum capacitors, with gaps far lower than 300 nm. Instead of using conventional resists that do not allow achieving such tight gaps, we employed very thin aluminum films. These act exactly as a resist since they are soluble in conventional developers. Pure TiN or TiN-based multilayers are then patterned into comb-shaped upper-electrodes onto the aluminum layer. The process ends with the dissolution of the sacrificial aluminum layer. This is achieved by a 60 min bath of the substrate in a basic developer, which slowly dissolves the aluminum layer and gently releases the upper-electrode. The comb-shape enhances the penetration and the diffusion of developers between electrodes and reduces the risk of collapse which can be significant if a single large electrode is used. To obtain superconducting suspended electrodes, we investigated three parameters: thickness, critical temperature and mechanical stress of the TiN layer forming the suspended electrode. Figure 4 shows measured stress and critical temperature T_c as a function of N_2 flow rate curve for 450 ± 50 nm-thick TiN layers deposited onto silicon substrates using Ar flow rate of 50 sccm at a total pressure of 0.6 Pa with a 700 W DC power.

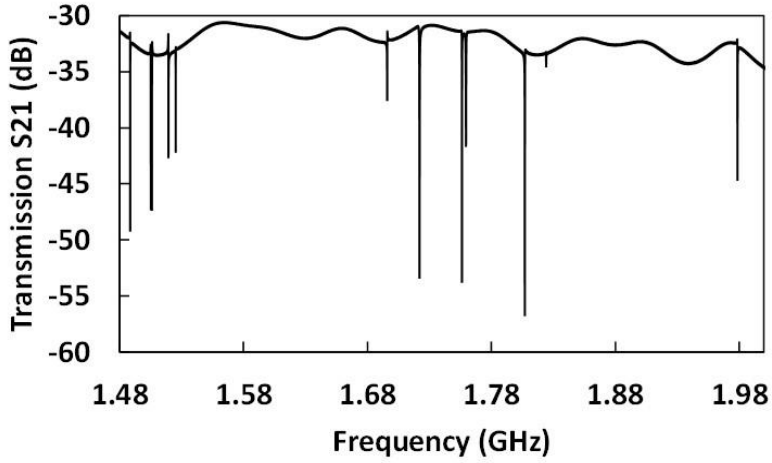

Fig. 6 Measured forward transmission S_{21} feedline of vacuum capacitor LEKIDs with power on feedline of -100 dBm, at 100 mK.

As reported elsewhere [16], the T_c versus N_2 flow curve shows a steep transition in T_c that occurs here at around 5 sccm. We evidence that this steep transition in T_c coincides with a peak in tensile stress. To achieve suspended bridges of typically $l_b \times w_b$ =30×10 μm, we found that they must be patterned from 400-600 nm-thick layers featuring a tensile stress ranging between ~200 and 600 MPa. Weaker (<200 MPa) or stronger (>600 MPa) tensile stress caused the electrodes to distort or break, whereas compressive stresses caused them to collapse. Unluckily, the ideal stress conditions coincide either with the steep transition in T_c or with a T_c lower than 200 mK. Thus, it is delicate to combine optimal stress and a suitable critical temperature with pure TiN. To address this issue, we fabricated electrodes made up of successive stoichiometric TiN layers (Tc~4.6K) and Nb layers (T_c~9 K). The Nb layer plays two roles: it increases the tensile stress, compensating the very low stresses of the stoichiometric TiN, and furthermore it increases the multilayer T_c through the proximity effect. The multilayer is made up of TiN/Nb/TiN/Nb~160nm/120nm/160nm/120nm. The TiN layer is first deposited to prevent inner surface oxidation. The 560 nm-thick multilayer shows a measured T_c of ~ 8.6 K and a tensile stress of ~ 530 MPa. TiN is deposited with a N_2 flow rate of 5.2 sccm. The Nb is deposited using the same parameters of the ones employed for the Nb-feedline. Using these parameters, we patterned different bridge sizes in order to insure that electrodes are not only suspended but also flat. This last point is particularly important to control

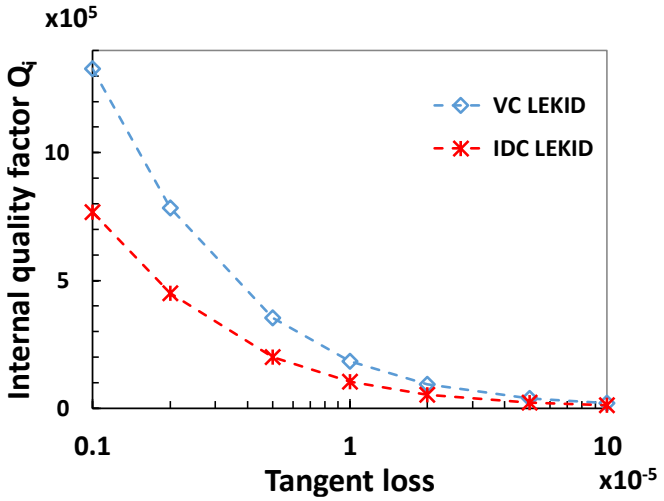

Fig. 7 Simulated internal quality factor of vacuum and interdigitated capacitor-based LEKIDs as a function of the substrate tangent loss ($tan\delta$).

the capacitance value. We noticed that large bridges (w_b>20 μm) tend to distort particularly at the edges. Ideally, the width w_b should range between 9 and 20 μm and the length should range between 32 and 35 μm. Figure 5-b shows a SEM picture of a typical vacuum capacitor achieved with the optimal geometry and fabrication parameters. Further observations using SEM revealed that almost all capacitors are well patterned (i.e. top electrodes are flat and well suspended).

4 Experimental results and discussion

The devices are mounted in a gold-plated copper box and wire bonded to two 50 Ω SMA connectors. They were cooled down to 72 and 300 mK by means of two fridges. The characterization consists in measuring the frequency noise and the forward transmission (S_{21}) to estimate the quality factors by fitting the resonances. Devices with 150 and 300 nm vacuum gap have been fabricated. The resonances are excited and measured through the feedline using a vector network analyzer. Out of the 25 resonators patterned we could observe 12 and 14 for respectively silicon and sapphire substrates, with resonating frequency between 1.48 and 1.97 GHz. The discrepancy between the high number of well-patterned vacuum capacitors, according to SEM pictures, and the number of measured resonances is probably due to Al residues between electrodes.

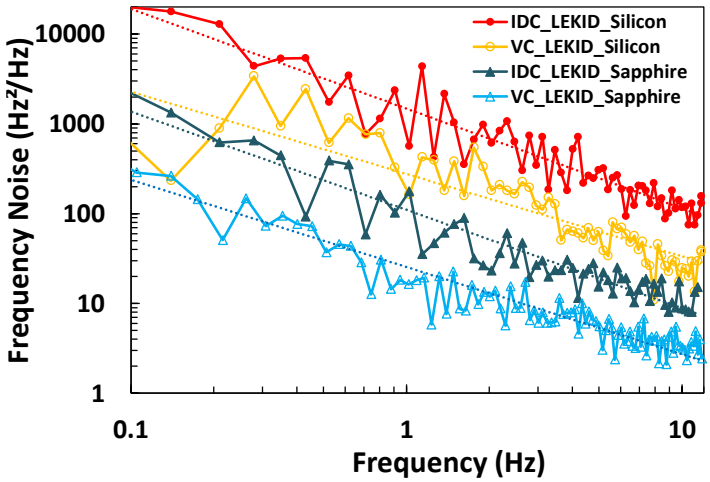

Fig. 8 Measured frequency noise of vacuum and interdigitated capacitor LEKIDs patterned respectively on silicon and sapphire substrates at 72 mK. For LEKIDs on sapphire substrate, we used resonances of: f_{VC_LEKID}=1.735 GHz (Q_i~3×10^5) and f_{IDC_LEKID}=1.327 GHz (Q_i~2×10^5). On silicon substrate: f_{VC_LEKID}=1.505 GHz (Q_i~2.4×10^5) and f_{IDC_LEKID}=1.321 GHz (Q_i~1.8×10^5).

Therefore, improving the release process of upper electrodes in the basic developer should increase the fabrication yield. The latter is higher for interdigitated capacitor LEKIDs, regardless of the employed substrate, with 29 out of 30 resonances observed between 1 and 1.45 GHz.

LEKIDs on silicon

Figure 6 shows the forward transmission (S_{21}) of the vacuum capacitor LEKIDs. The highest internal quality factor Q_i~4.3×10^5 is obtained when the lowest power, of around -115 dBm, is applied on the feedline, leading to the raw estimation of the tangent loss [14] $tan\delta_i = 1/Q_i$~2.3×10^{-6}. The coupling quality factor is Q_c~2.2×10^4. The internal quality factors Qi measured in similar conditions for the interdigitated capacitor LEKIDs are lower. We obtained a maximum of Q_i~2×10^5 and thus $tan\delta_i$~5×10^{-6}. The coupling factor is Q_c ~2×10^4. When a higher readout power is applied, typically about -110 dBm, we noticed that the internal quality factor Q_i of the vacuum capacitor LEKIDs on silicon, instead of increasing as usually reported [5][8][9], decreases to 1.6×10^5, whereas it increases (as expected) up to ~3×10^5 for the interdigitated capacitor LEKIDs at -70 dBm. This behaviour is unclear and

further investigations are being carried out. The slight difference in Q_i between the two geometries is probably due to the losses in the silicon substrate as predicted by simulations, see Fig. 7. To assess the substrate loss effect on quality factors for both geometries, we performed simulations where the tangent loss is varied between 10^{-6} and 10^{-4}. For weak losses (small $tan\delta$), Q_i further improves for both geometries but with different amounts: the weaker the $tan\delta$, the larger the Q_i difference between the two geometries. For large $tan\delta$ approaching 10^{-4}, Q_i degrades and tends toward the same value for the two geometries. This can be easily explained by the fact that the substrate loss effects concern the whole interdigitated capacitor resonator whereas it is located only in the meander part for the vacuum capacitor LEKID. In other words, the use of a vacuum capacitor certainly improves the quality factor of LEKIDs but as losses arise also elsewhere, its effect tends to vanish for high losses. The losses are likely caused by residue or new native oxides formed on the substrate. This relative improvement in Q_i is also observed in frequency noise measurements. Figure 8 presents the frequency noise measured at 72 mK. Interdigitated capacitor LEKIDs feature a high frequency noise of 123 ± 43 Hz²/Hz at 10 Hz which is nevertheless on par with the best value reported in [17] for the same test bench. The vacuum capacitor LEKIDs feature a much lower noise of 24 ± 12 Hz²/Hz at 10 Hz.

LEKIDs on sapphire

The largest internal quality factor of Q_i~1.1×10^6 is achieved with vacuum capacitor LEKIDs on sapphire substrate. This translates into a tangent loss $tan\delta_i = 1/Q_i$ of ~9×10^{-7}. The coupling factors is Q_c~2×10^4. Interdigitated capacitor LEKIDs on sapphire exhibit a maximum Q_i of ~3.1×10^5 and a coupling factor of Q_c~2.8×10^4. Very low noise of 2.8 ± 0.5 Hz²/Hz is achieved with vacuum capacitor LEKIDs, whereas 16 ± 6 Hz²/Hz is measured for interdigitated capacitor LEKIDs. Thus, as it has also been demonstrated elsewhere using coplanar resonators [18], the sapphire substrate features lower losses which allowed, on the one hand, to further improve Q_i of resonators, corroborating the simulation results of Fig. 7, and, on the other hand, to lower the noise level for both geometries. To experimentally estimate parasitic capacitors within the resonator, we fully removed the vacuum capacitors by destroying the upper-electrodes. Using $C_0'/C_0 = (f_0/f_0')^2$, where C_0 is the total capacitor and C_0' is the parasitic capacitor, it turns out that the total capacitor is made up of ~48% of vacuum capacitors and ~52% of parasitic capacitor confirming the simulation result. This demonstrates that the meander part in LEKIDs is probably an important source of noise likely

through its intrinsic capacitors. Internal and coupling quality factors of destroyed vacuum capacitor resonators degrade slightly as we measure $Q_i \sim 1.8\times10^5$ and $Q_c \sim 1.4\times10^4$, respectively, when a similar power on the readout line is applied. According to Sonnet simulations, the decrease in Q_c is caused by the change of the coupling strength between the resonator and the feedline when the capacitor is destroyed. Indeed, the most important coupling is achieved through the meander but also through the entire resonator, including the capacitor, through the surrounding ground plane. It is worth noting that all these experimental results are in good agreement with the simulations.

5 Summary

In summary, we have successfully developed TiN vacuum capacitor-based LEKIDs. To accomplish this, we implemented an innovative and straightforward process to build vacuum gaps where instead of using conventional resists, we employed a thin Al film as sacrificial layer. A comparative study between vacuum capacitor LEKIDs and classical interdigitated capacitor LEKIDs demonstrates that, unlike what is usually reported, the meander part can be an important source of noise, as important as the capacitor part. This is probably a consequence of its parasitic capacitance, and must be taken into account for future designs. However, compared to interdigitated capacitors, vacuum capacitors allowed us to improve the internal quality factor and reduce the noise in our LEKIDs. Besides, we also demonstrated and confirmed that sapphire substrates are better than silicon ones to build low noise kinetic inductance detectors. Thus, an ultimate sensitivity can be achieved with TiN LEKIDs featuring a weak meander volume along with a large vacuum capacitor patterned on a sapphire substrate. These vacuum capacitors are also suitable for other applications such as quantum computers and superconducting parametric amplifiers.

References

1. J. Gao et al.,Appl. Phys. Lett. 92, 152505 (2008).
2. O. Noroozian et al., AIP Conf. Proc. 1185, 148–151 (2009).
3. P. K. Day et al., Nature 425 (6960), 817–821 (2003).
4. J. M. Martinis et al., Phys. Rev. Lett. 95, 210503 (2005).
5. S. J. Weber et al., Appl. Phys. Lett. 98, 172510 (2011).
6. H. Paika and K. D. Osborn, Appl. Phys. Lett., 96, 072505 (2010).

7. D. P. Pappas et al., IEEE Trans. on Appl. Supercond., Vol. 21, No. 3, June 2011.
8. K. Cicaket al.,Appl. Phys. Lett., 96, 093502 (2010).
9. A. D. O'Connellet al., Appl. Phys. Lett. 92, 112903 (2008).
10. S. Beldi et al., J. Low Temp. Phys. 193:184-188 (2018).
11. S. Beldi et al., Vol. 27, No. 9, Optics Express 13319, 2019.
12. http://www.sonnetsoftware.com.
13. S. Ariyoshi et al., Applied Physics Express 6 (2013) 064103.
14. M. S. Khalil et al., IEEE Trans. Appl. Supercond. , Vol. 21, No. 3, June 2011.
15. B. Mazin, AIP Conference Proceedings 1185, 135 (2009).
16. H. G. Leduc et al., Appl. Phys. Lett. 97, 102509 (2010).
17. G. Coiffard et al., Journal of Low Temperature Physics, August 2016, Vol. 184, Issue 3–4, pp 654–660.
18. B. Mazin, Microwave Kinetic Inductance Detectors, Ph.D. thesis, California Institute of Technology (2004).